Neonatal hemodynamic response to visual cortex activity: high-density near-infrared spectroscopy study

Steve M. Liao
Washington University School of Medicine
Department of Pediatrics
and
Department of Neurology
and
Department of Radiology
St. Louis, Missouri 63110

Nick M. Gregg
Washington University School of Medicine
Department of Radiology
St. Louis, Missouri 63110

Brian R. White
Washington University School of Medicine
Department of Radiology
and
Washington University
Department of Physics
St. Louis, Missouri 63130

Benjamin W. Zeff
Katelin A. Bjerkaas
Washington University School of Medicine
Department of Radiology
St. Louis, Missouri 63110

Terrie E. Inder
Washington University School of Medicine
Department of Pediatrics
and
Department of Neurology
and
Department of Radiology
St. Louis, Missouri 63110

Joseph P. Culver
Washington University School of Medicine
Department of Radiology
and
Washington University
Department of Physics
St. Louis, Missouri 63130

Abstract. The neurodevelopmental outcome of neonatal intensive care unit (NICU) infants is a major clinical concern with many infants displaying neurobehavioral deficits in childhood. Functional neuroimaging may provide early recognition of neural deficits in high-risk infants. Near-infrared spectroscopy (NIRS) has the advantage of providing functional neuroimaging in infants at the bedside. However, limitations in traditional NIRS have included contamination from superficial vascular dynamics in the scalp. Furthermore, controversy exists over the nature of normal vascular, responses in infants. To address these issues, we extend the use of novel high-density NIRS arrays with multiple source-detector distances and a superficial signal regression technique to infants. Evaluations of healthy term-born infants within the first three days of life are performed without sedation using a visual stimulus. We find that the regression technique significantly improves brain activation signal quality. Furthermore, in six out of eight infants, both oxy- and total hemoglobin increases while deoxyhemoglobin decreases, suggesting that, at term, the neurovascular coupling in the visual cortex is similar to that found in healthy adults. These results demonstrate the feasibility of using high-density NIRS arrays in infants to improve signal quality through superficial signal regression, and provide a foundation for further development of high-density NIRS as a clinical tool. [DOI: 10.1117/1.3369809]

Keywords: biomedical optics; imaging systems; infrared imaging.

Paper 09286R received Jul. 8, 2009; revised manuscript received Jan. 14, 2010; accepted for publication Jan. 26, 2010; published online Apr. 30, 2010.

1 Introduction

The survival rate of preterm infants has improved dramatically in recent decades due to advances in perinatal and neonatal care. However, the neurodevelopmental outcome of NICU infants remains a major clinical concern, with a significant proportion displaying cognitive and behavioral deficits during childhood.[1] The ability to noninvasively assess neural function may provide early recognition and evaluation of cerebral dysfunction in high-risk infants, enabling targeted early intervention. Functional neuroimaging is commonly performed using hemodynamic contrasts [e.g., functional MRI (fMRI) or near-infrared spectroscopy (NIRS)], in which local neural activity is mapped through the neurovascular response. While fMRI is the most widely used technique in adults and has a well-established methodology, its disadvantages include

Address all correspondence to: Joseph P. Culver, Ph.D, Washington University School of Medicine, Department of Radiology, 4525 Scott Avenue, East Building, Room 1137, Campus Box 8225, St. Louis, Missouri 63110. Tel: 314-747-1341; Fax: 314-747-5191; E-mail: culverj@wustl.edu

1083-3668/2010/15(2)/026010/9/$25.00 © 2010 SPIE

potential safety concerns in transporting unstable infants to the fixed scanner, indirect surrogates of hemodynamics [e.g., blood oxygenation level dependent (BOLD) signal], low temporal resolution, and high cost. NIRS is an alternative neuroimaging modality with the advantages of portability, low cost, and more comprehensive hemodynamic contrasts.[2,3] These benefits may allow NIRS systems to be used for longitudinal, bedside clinical monitoring of neonatal brain function.

Despite its inherent advantages, the clinical application of NIRS has been limited by technological challenges. Stringent instrumentation requirements have restricted the ability to distinguish cerebrovascular signals from superficial hemodynamic signals arising from scalp and skull. Recently, a tomographic approach using high-density NIRS imaging arrays has been shown to provide improved measurements of brain function in adults.[2,4–6] The high-density fiber arrangement also provides multiple distance measurements within the array, therefore allowing a regression approach to minimize spurious or systemic signals contaminating true cerebral signals. In this study, we aim to extend the use of our high-density NIRS arrays[2] to evaluate healthy term-born infants.

The extension of functional neuroimaging (for fMRI or NIRS) to infants has been hindered by a lack of understanding about the neurovascular coupling linking neural activity to the hemodynamic response. In the healthy, mature brain, increased neural activity drives an increase in both cerebral blood volume (CBV) and tissue oxygen saturation (StO_2). In healthy adults, the balance of these two factors results in a net localized decrease in deoxyhemoglobin (HbR): a "positive BOLD response."[7,8] When this balance is altered (e.g., due to injury), stimulation may result in "negative BOLD responses."[9–13] During early development, the brain's metabolism is complex and varying, resulting in the possibility of an immature neurovascular coupling.[14] fMRI studies of infants have found both negative and positive BOLD responses in response to sensory stimuli.[15–20] In contrast to BOLD-fMRI, NIRS can measure oxy- (HbO_2), deoxy- (HbR),[21] and total hemoglobin (HbT), providing a more comprehensive view of brain metabolism,[22–24] even in situations of altered neurovascular coupling. HbT provides a relatively robust indicator of CBV, while the ratio of HbO_2 and HbT reflects StO_2. In addition to imaging technique issues, previous NIRS and fMRI studies of infants have also suffered from a broad range of study protocols (e.g., a diversity of stimulus conditions, sleep/sedation states, and ages). Thus, the nature of the cerebral hemodynamic response to increased neural activity in healthy infants remains unclear.

In this study, we constrain the stimulus protocol variables by evaluating a relatively well-studied sensory stimulus (visual) within the first three days of life in healthy term infants. This study provides the youngest cohort of subjects in which the hemodynamic response to visual stimulation has been assessed. This feasibility study of high-density NIRS and investigation of the healthy neonatal hemodynamic response intends to strengthen the foundation for the development of NIRS as a clinical tool.

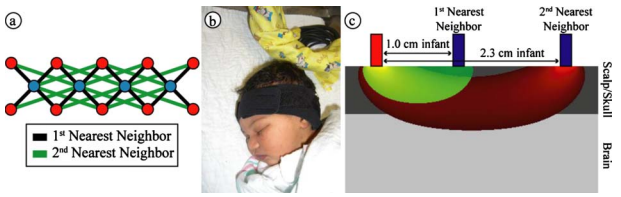

Fig. 1 High-density scanning grid on an infant subject. (a) Schematic of our high-density scanning grid. Blue dots are light source positions; red dots are detector positions. Each detector is capable of distinguishing light signals originating from multiple source positions (the interconnecting lines). (b) Visual response data being taken on a sleeping baby. The LCD screen is typically placed 20 cm away from the infant's face (not shown). Observe the soft neoprene cap and flexible optical fibers placed over the occipital cortex. (c) A schematic diagram showing a detector and two source positions arranged 1 and 2.3 cm apart. Note that signals coming from the 1-cm source position likely sample tissue from the superficial layer of the head, while signals from the second-nearest source position likely sample tissues from a combination of superficial and brain tissues. (Color online only.)

2 Methods

2.1 *Subjects*

Healthy infants who were products of term pregnancies were recruited from the postnatal wards at Barnes-Jewish Hospital (Saint Louis, Missouri). The study protocol was approved by the Human Research Protection Office of the Washington University in Saint Louis School of Medicine. Written informed consent was obtained from the parents prior to each study.

2.2 *Instrumentation*

We previously developed a multichannel, continuous-wave, high-density diffuse optical imager for use in adults.[2] The simple and modular instrumentation made it easily scalable to a portable system for bedside use in the nursery. For this study, we assembled a system with 13 source positions and 15 detector positions. Each source position consisted of two near-infrared wavelengths (750 and 850 nm) of light emitting diodes (LEDs). Each detector position had a dedicated avalanche photodiode and analog-to-digital converter. Light was carried to and from the scalp via flexible optical fibers with a diameter of 2.5 mm (optodes). The optodes were held onto the scalp by a silicone pad, an elastic neoprene band, and hook-and-loop strapping. For recording over the visual cortex, we arranged fibers in a high-density 4×10 configuration of four sources and ten detectors [Fig. 1(a), overall dimensions 2×6 cm]. For recording simultaneously over the motor cortex, we assembled a second similar pad with a 7×5 configuration.

2.3 *Protocol*

We used the inion (the bony prominence over the back of the head) as our landmark for the position of the visual cortex and for imaging pad placement. The visual cortex imaging pad was positioned over the inion and held on with the strap positioned over the forehead [Fig. 1(b)]. All measurements were taken within 2 h after feeding in a dimly lit room with the intent of imaging the infants while in a quiet state with eyes

closed. Previous studies using both NIRS and MRI have shown that light can sufficiently penetrate closed eyelids in both adults and infants to induce a measurable hemodynamic response over the visual cortex.[25,26] Visual stimulation was provided by a 19-in.-liquid crystal display (LCD) monitor at a distance of 20 cm from the infant's face. The screen was placed over the top of the bassinet if the infant was lying supine. If the infant preferred to lie on the side, then the screen was swung to the side of the bassinet. The stimulus consisted of two counterphase checkerboard patterns (total luminance 50%) and a 0% flat luminance pattern. A full cycle of four frames (checkerboard, flat, counterphase checkboard, and flat) was displayed once every second. The checkerboard pattern was not necessary for the current study, since with the eyes closed only the luminance changes are detected. However, we employed the checkerboard pattern with anticipation of parallel studies of awake infants that are not part of this study. Ten seconds of stimulus was followed by a black screen for 20 s. This cycle was repeated for 15 to 20 min, depending on how long the infant remained reasonably still. In two subjects, the sensorimotor cap was added to the visual cap with a neoprene strap across the top of the head, and data were taken simultaneously. One of these subjects was used as a negative control (the only stimulus was a blank screen) and the other viewed the standard visual stimulus, with the sensorimotor pad acting as an internal control. To confirm that the well-established healthy adult neurovascular coupling can be obtained using our system, we acquired data from the visual cortex of a 26 year-old healthy female.

2.4 *Data Analysis*

Source-detector pairs (channels) were processed individually. We took the logarithm of the ratio of each channel's level (l_j) to its mean ($\langle l_i \rangle$), which yielded time traces of the differential light intensity $y_i = -\log(l_i/\langle l_i \rangle)$ for each wavelength. Each channel was high-pass filtered (0.02 Hz) to remove long-term drift, and low-pass filtered (0.5 Hz) to remove high-frequency noise and pulse artifact. Source-detector (SD) pairs with 1-cm separation [first-nearest neighbors, Fig. 1(a)] are primarily sensitive to the scalp and skull, but not the brain. A systemic/superficial noise signal is modeled by spatially averaging the first-nearest neighbor signals:

$$y_n = (1/N_{nn}) \sum_{j=1}^{N_{nn}} y_j .$$

Here, y_j are first-nearest neighbor pair measurements, N_{nn} is the number of first-nearest neighbors in the array, and y_n is the superficial noise signal. The contribution of this noise signal to all measurements is removed by regression: $y_{i,\mathrm{brain}} = y_i - \alpha_i y_n$, where α_i is a temporal correlation factor $\alpha_i = \langle y_i, y_n \rangle / \langle y_n, y_n \rangle$, y_i is the unmodified SD pair time course, and $y_{j,\mathrm{brain}}$ is the SD pair after superficial signal regression. Here the brackets $\langle a, b \rangle$ indicate calculation of the correlation coefficient between two time courses a and b. The resulting measurements more accurately reflect the true brain hemodynamics.[2,27] The performance of this regression procedure was evaluated by comparing the contrast-to-noise ratio of the activation responses with and without regression.

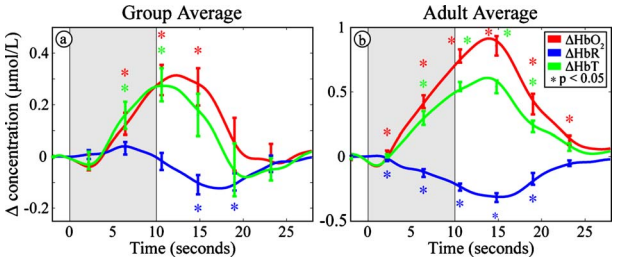

Fig. 2 Hemodynamic changes in response to visual stimulation (HbO_2: red, HbR: blue, and HbT: green). The shaded gray areas denote our 10-s visual stimulus. Error bars show mean and standard error for each five second interval. Asterisks show points that are significantly ($p < 0.05$) different from baseline using a two-tailed t-test. (a) Hemodynamic response (averaged across eight infants) showing significant increases in HbO_2 and HbT and a significant decrease in HbR. (b) Hemodynamic changes in response to visual stimulation in a single healthy young adult, showing the same pattern. (Color online only.)

The log-ratio data ($\Delta y_{j,\mathrm{brain}}$) are converted to changes in absorption using the modified Beer-Lambert law. The differential path length factors (DPFs, which account for the longer path taken by scattered photons) used were 5.11 and 4.67 for 750 and 850 nm, respectively.[28] The relative absorption changes at the two wavelengths were converted to concentration changes in the two hemoglobin species using their extinction coefficients. We used extinction coefficients for HbO_2 of 1.39 and 3.31 $mM^{-1}*cm^{-1}$ and for HbR of 2.49 and 1.84 $mM^{-1}*cm^{-1}$ at 750 and 850 nm, respectively. These coefficients were generated using the table in Wray, Cope, and Delpy,[29] with a weighted average over the Gaussian LED spectrum. HbT was found by summing HbO_2 and HbR.

Stimulus blocks with high standard deviations (>3% temporally) were considered corrupted by motion artifacts and excluded from further analysis. The remaining blocks were averaged to create a response time trace for each infant. While selecting blocks with activations would provide stronger activation responses, we did not do this, since it can also bias the sign of the block-averaged data. All of the results displayed are averaged from second-nearest neighbor measurements (separation 2.3 cm), which are more sensitive to the brain. This pad-averaged signal, while not localizing the response, is a reasonable approach, since we expect the response to be bilateral.

For statistical analysis, hemoglobin time traces were down-sampled to 0.2 Hz (5-s intervals). Since the peak changes occur at different times for the different contrasts, we analyzed the statistical significance at the time of the peak signal for each contrast separately. The changes at the peak were compared to the five-second baseline around stimulus onset using a Student's t-test. The t-statistic was converted to a p-value using both tails of the distribution (i.e., no directionality to the response was assumed). Significance was inferred for all p-values less than an α of 0.05.

3 Results

We recruited a total of 11 healthy (five male and six female) full-term neonates during the first three days of life. The mean gestational age of the infants was 39 5/7 weeks (range

Table 1 Clinical characteristics for each study subject. (M=male; F=female; C/S=Cesarean-section; Vag=vaginal delivery; C=Caucasian; B=Black).

ID	Gender	Gestational age at birth (weeks)	Age at scan (days)	Mode of delivery	Race
1	M	37 2/7	2	C/S	C
2	F	38 4/7	3	C/S	C
3	M	37 2/7	2	Vag	B
4	F	40 6/7	2	C/S	C
5	F	41 1/7	2	Vag	B
6	M	39 5/7	2	Vag	B
7	M	40 6/7	2	Vag	B
8	F	41 0/7	1	Vag	C
9	F	39 6/7	2	C/S	C
10	F	40 3/7	1	Vag	B
11	M	39 6/7	1	Vag	B
Mean	—	39 5/7	2	—	—

37 1/7 to 41 1/7 weeks), and the mean postnatal age at the time of the scan was 2 days (range 1 to 3 days). The prenatal and postnatal courses were uncomplicated for all of these infants. Each infant was examined by a physician and none showed any abnormal findings. The clinical details of the subjects are outlined in Table 1. The presence of the cap did not disturb the infants, and all infants laid quietly with eyes closed (visual inspection by data collectors) during the scanning session [as in Fig. 1(b)]. Infant 3 was excluded from analysis due to significant noise, likely due to excessive motion (strong pacifier sucking was observed). Of the remaining ten infants, eight were imaged with the standard visual cap and stimulus. The final two were imaged with the combined motor and visual cap, and their data are presented separately.

In the eight infants who were presented with the visual stimulus, we found the same hemodynamic response pattern: increases in oxyhemoglobin (HbO_2) and total hemoglobin (HbT) and a decrease in deoxyhemoglobin (HbR). The hemodynamic response averaged across all selected blocks from all infants is shown in Fig. 2(a). Note the number of statistically significant deviations from baseline. For comparison, Fig. 2(b) shows the typical hemodynamic response measured in a single healthy adult. The results for each infant individually are shown in Table 2. The peak changes were significant in HbO_2 for six of eight infants, in HbR for four of eight infants, and in HbT for five of eight infants. The mean HbO_2 peak was 0.28 ± 0.16 μmol/L ($\pm$ standard deviation), the mean HbT peak was 0.27 ± 0.18 μmol/L, and the mean HbR trough was -0.11 ± 0.11 μmol/L. Note that since the peak changes occur at different times, the sum of the peak values for HbO_2 and HbR do not equal the peak values for HbT. The last three columns (5, 6, and 7) of Table 2 detail the ratio between the contrast-to-noise ratio (CNR) in the data with and without superficial signal regression of the data. The CNR improvements are evident in all three contrasts.

In the infant scanned with the additional sensorimotor cap and presented with the visual stimulus, the visual cortex showed the same changes as noted in the other infants [Fig. 3(a)], while the sensorimotor region showed no significant changes [Fig. 3(b)]. In the infant scanned without the presentation of a stimulus, neither the visual [Fig. 3(c)] nor the sensorimotor cap [Fig. 3(d)] showed any significant changes.

To determine whether the regression step improved the time courses, we also processed the data without the regression step (Fig. 4). With regression, the average contrast of the eight infants is 0.35, −0.15, and 0.29 μmol/L for HbO_2, HbR, and HbT, respectively; noise (standard error) is 0.080, 0.055, and 0.11 μmol/L; and contrast to noise is 3.8, 3.2, and 2.5. Without regression, the contrast is 0.50, −0.22, and 0.45 μmol/L for HbO_2, HbR, and HbT, respectively; noise (standard error) is 0.45, 0.17, and 0.53 μmol/L; and contrast to noise is 1.9, 2.7, and 1.5. Although there is a modest attenuation of the contrast, the regression provided a significant increase in the contrast-to-noise ratio due to the reduction of noise. The attenuation of the contrast is further considered in the discussion.

4 Discussion

Previously, we have shown the benefits of high-density imaging arrays in adults. In this feasibility study, we aimed to establish the feasibility of using high-density arrays in infants. A challenge of working with high-density arrays is the bulk of the many fibers. Therefore, we did not start with a full-size imaging pad (e.g., 24 sources $\times$28 detectors) as used with adults. Rather, we retained the high-density spatial sampling (1 cm) but worked with a smaller field of view (4 sources $\times$10 detectors). This amount of fibers was sufficient to cover the visual cortex region and permitted testing of one benefit of high-density arrays: the use of first-nearest neighbor measurements for a superficial signal regression procedure. The 4 $\times$10 array used over the visual cortex permits 16 measurements with 1-cm SD-pair distances and 12 measurements with 2.3-cm distances. For reference, recent related work by Karen et al. recording infant visual responses used an array with eight measurements at 2.5-cm distances and two measurements at 3.75 cm. Thus, the current 4$\times$10 array has optodes packed over three times more densely (per unit area) than the Karen et al. array. This higher-density arrangement, with the shortest distance being 2.5$\times$ shorter and more specific to the scalp, facilitates the regression procedure. Finally, the fibers are arranged in a manner that supports future imaging experiments.

Our results demonstrate the feasibility of using high-density arrays of fibers to record brain activity in infants. The signal levels were sufficient in all nine infants to record from multiple source-detector distances. Of these nine infants, we were able to record with sufficient signal-to-noise ratio to detect visual activations in eight. The regression procedures provided up to a 2.9$\times$ improvement in contrast-to-noise ratio of the responses (in HbO_2) to visual activations. Assuming that the competing noise is random, this CNR improvement trans-

Table 2 Average change and standard error in oxy-, deoxy-, and total hemoglobin concentrations in response to visual stimulation for each study subject. Deviations that are statistically different ($p < 0.05$) from baseline are marked with an asterisk. The group mean and standard deviation of the mean are also shown. The effect of SSR on CNR is given for each individual. The group mean and standard deviation of the mean are also shown.

ID	ΔHbO_2 (μmol/L) mean (SE)	ΔHbR (μmol/L) mean (SE)	ΔHbT (μmol/L) mean (SE)	ΔHbO_2 $10\times\log_{10}$(SSR/raw) CNR	ΔHbR $10\times\log_{10}$ (SSR/raw) CNR	ΔHbT $10\times\log_{10}$ (SSR/raw) CNR
1	+0.34* (0.09)	−0.096 (0.12)	0.38 (0.20)	6.71	11.30	3.93
2	+0.46* (0.075)	−0.17* (0.053)	0.47* (0.12)	3.22	−0.969	3.50
4	+0.20* (0.067)	−0.023 (0.041)	0.22 (0.091)	8.44	−5.09	14.9
5	+0.54* (0.12)	−0.15* (0.04)	0.43* (0.13)	3.83	2.58	3.14
6	+0.55* (0.10)	−0.31* (0.039)	0.41* (0.077)	0.0860	0.00	0.792
7	+0.41* (0.12)	−0.20* (0.035)	0.32* (0.11)	0.828	6.17	1.04
8	+0.13 (0.09)	−0.13 (0.056)	0.0075 (0.079)	5.85	1.30	−2.76
9	+0.16 (0.083)	−0.11 (0.056)	0.089 (0.095)	7.69	−0.458	−0.0436
Mean (SD)	+0.35 (0.17)	−0.15 (0.08)	0.29 (0.17)	4.58 (3.10)	1.85 (4.98)	3.06 (5.26)
				4.69 w/o max and min (2.54)	1.44 w/o max and min (2.65)	2.06 w/o max and min (1.66)

lates to an approximately 8× reduction in the time needed to obtain similar contrast-to-noise ratios between the two approaches. Since the influences of superficial variations have been largely removed from the measurements, the resulting signals interrogate the brain with greater specificity. While we do not know the shape of the hemodynamic response *a priori*, we note that qualitatively the general shape of the regressed hemodynamic response is smoother and more similar to the response that would be expected from adults. This method therefore provides increased confidence in the data quality and the characterization of the hemodynamic response compared to traditional single-distance NIRS recordings. Finally, these results provide a basis for advancing future studies with a large-scale imaging pad.

Our results also demonstrate that in quiet resting, healthy term-born infants in the first three days of life, with eyes closed, the visual cortex responds to visual stimulation by an increase in HbO_2 and HbT and a decrease in HbR. Our data also indicate that the observed response is specific to the visual stimulus and localized to the occipital region. No periodic systemic fluctuation was observed during the extended resting period without visual stimulation. The similarity of the response in the infants indicates the robustness of the measurement and the high reliability of our system within the neonatal population.

Our results are comparable to those from a recent study published by Karen et al.,[30] in which they found a mean HbO_2 increase of 0.98 μmol/L and a mean HbR change of −0.17 μmol/L in a group of 20 healthy term infants with a mean age of 5.5 days. One difference between the analyses is that the assumed differential path length factors (DPFs) are not the same. Karen et al. applied a DPF the value of 4 from the results by Wyatt et al.,[31] which used whole-head time-of-flight measurements taken up to three days postmortem from premature infants who died of intraventricular hemorrhage. In our study, we elected to use the DPF formulas reported by Duncan et al.,[28] as they used both living infants and had a reflectance measurement geometry similar to our own. Uncertainty in the DPF values can lead to errors in the magnitude of the hemodynamic response. Ideally, these DPF values and/or the optical properties of the head would be measured individually for each subject. For instance, the optical properties were recently measured using frequency-domain NIRS (FD-

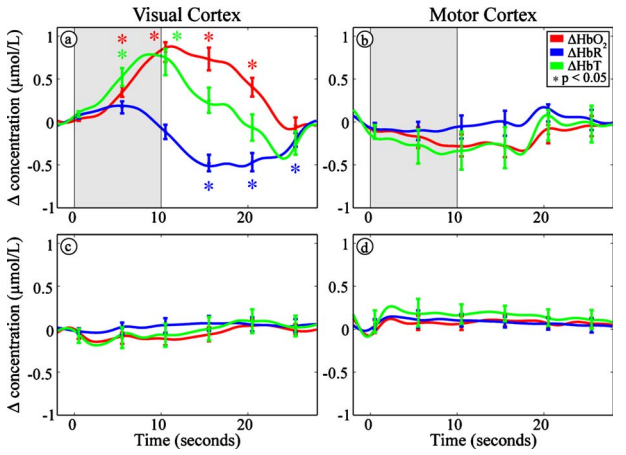

Fig. 3 The hemodynamic response is specific to both the visual stimulus and the occipital region (HbO_2: red, HbR: blue, and HbT: green). The shaded areas denote our visual stimulus. Error bars show mean and standard error for each five second interval. Asterisks show points that are significantly ($p<0.05$) different from baseline using a two-tailed *t*-test. (a) and (b) Hemodynamic measurements in a single baby with simultaneous recording from both visual and sensorimotor cortices, showing a hemodynamic response in the visual but not the sensorimotor cortex. (c) and (d) Hemodynamic measurements taken from both visual and somatosensory cortices during 10 min of rest without a visual stimulus. Note the lack of any functional response. (Color online only.)

NIRS) in a large group of infants longitudinally.[32,33] Though functional responses were not measured in the FD-NIRS study, the results demonstrated the feasibility of measuring the *in-situ* optical properties, which could, in principal, be combined with the activation measurements detailed here.

An additional potential confound in evaluating the ratio of HbO_2 to HbR is cross talk between HbO_2 and HbR due to noise in the spectroscopy. Strangman, Franceschini, and Boas showed that the 780/830-nm pairing is susceptible to this problem.[34] However, due to the peak in HbR absorption at 760 nm, the 750/830-nm pairing appears more robust.[35] Here we use 750/850 nm, and in the Karen et al. study, they used 730/830 nm, which minimizes this issue.

As in the study of Karen et al., while six of eight of our infants showed significant increases in HbO_2, fewer infants (four) showed significant decreases in HbR. Further, the ratio of the group-averaged contrast over the standard deviation was superior for HbO_2 (2.0) than for HbR (1.4). Thus, our results reinforce their conclusion that HbO_2 is a "more reliable indicator of functional activity than [HbR] or BOLD signal."[30] While we found a similar response between healthy adults and infants, discrepancies in the visual activation response between different ages of infants and adults have been reported in previous studies. The pattern found in healthy adults (i.e., increased HbO_2 and decreased HbR) has been previously reported in infants by both Taga et al. [36] and Karen et al.[30] In contrast, Meek et al.[37] found an increase in both HbO_2 and HbR. This controversy in neurovascular coupling is also reflected in the literature from BOLD-fMRI studies. Born et al.[15] found that in sedated or sleeping infants, there was a decrease in BOLD signals in response to visual stimulation, whereas in adults, there was an increase in BOLD signals. Yamada et al.[20] and Martin et al.[38] both showed an interesting dichotomy: younger infants showed the typical adult pattern of BOLD signal increase, whereas older infants showed a BOLD signal decrease in the visual cortex, while the oldest infants returned to a positive BOLD response. The timing of these changes varied between the two studies, with the first transition occurring at 8 weeks of age in the infant cohort from Yamada et al., and at 16 weeks in those from Martin et al.; the latter transition was observed at 40 months in Martin et al. with negative BOLD responses peaking at 1 to 2 years of age. A summary of the study methodologies and results is presented in Table 3.

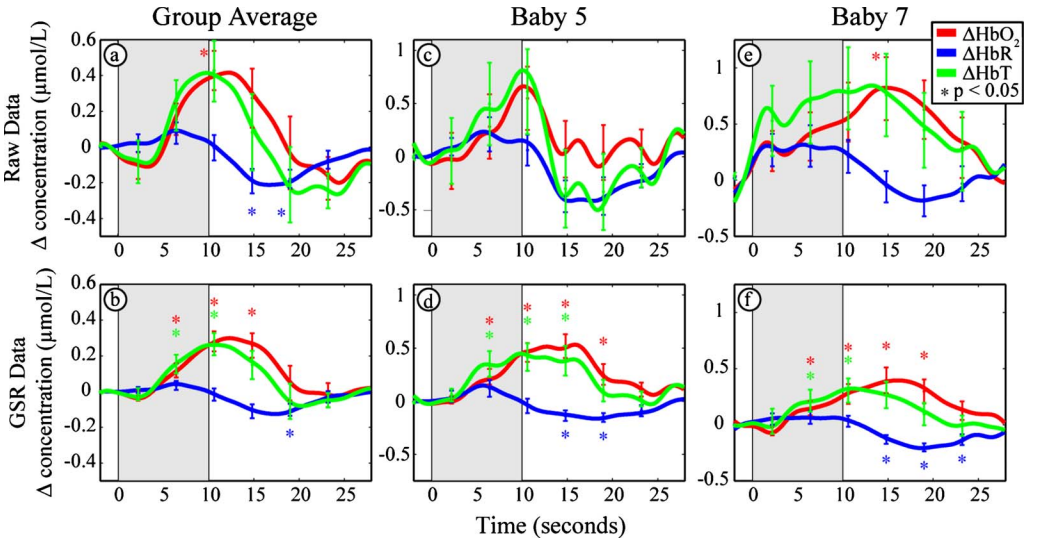

Fig. 4 Evaluation of the superficial signal regression (SSR) in infants. Raw data (a), (c), and (e) without the application of SSR show wide fluctuations (i.e., standard error bars) in all three measured parameters (i.e., oxy-, deoxy-, and total hemoglobin concentration changes). After the application of the SSR method to the same dataset (b), (d), and (f), moderate improvements are observed in the signal strengths, but significant reductions in noise levels (as shown by the standard error bars) are evident compared to the raw dataset.

Table 3 Summary of the literature on hemodynamic responses in infants. Papers from the same investigators are grouped into single rows.

Reference	Method	Age	State	Stimulus	Result
20 44 25	BOLD-fMRI	0 to 32 Weeks	Pentobarbital sedation	8-Hz stroboscopic light	↑BOLD ⩾ 7 wk, ↓BOLD ⩽ 8 wk
16	BOLD-fMRI	3 days to 48 months	Asleep, older children sedated with chloral hydrate	8-Hz stroboscopic light	↓BOLD
38	BOLD-fMRI	1 day to 12 years	General anesthesia 0.5% halothane in mix of N_2O:O_2, chloral hydrate, pentobarbital	8-Hz red LED goggles	↓BOLD, ↑BOLD, or no change
45	BOLD-fMRI	18 months	Promethazine, pehidine, droperidol	8-Hz red LED goggles	10 no change 1 ↑BOLD 17 ↓BOLD
46	BOLD-fMRI	2 months to 9 years	Penthbarbital or chloral hydrate	8-Hz LED goggles	↓BOLD
36 47	NIRS	2 to 4 months	Awake	4-Hz reversing checkerboard	↑HbO_2, ↓HbR
30	NIRS	2 to 9 days	Asleep	1-Hz Red LED goggles	↑HbO_2, ↓HbR
37	NIRS	3 days to 14 weeks	Awake	5-Hz reversing checkerboard	↑HbO_2, ↑HbR
48	NIRS	4 to 5 days	Asleep	10-Hz stroboscopic light	↑HbO_2 and ↑HbR ↓HbR, or no change in HbR
26	NIRS	29 to 111 days	Asleep	8-Hz stroboscopic light	↓HbO_2, ↑HbR
This work	High-density NIRS	1 to 3 days	Asleep	2-Hz LCD checkerboard	↑HbO_2, ↓HbR

Another consideration when analyzing the literature on infant neurovascular coupling is that many BOLD-fMRI studies are often conducted with the infants under sedation to prevent movement. Multiple studies have found effects on the BOLD response due to anesthesia, including nonlinear and nonmonotonic dose-response curves.[39] Cannestra et al. found that pentobarbital in adults caused negative BOLD responses to visual stimulation.[40] Thus, interpretation of findings from sedated infants using BOLD-fMRI is complex. In contrast, NIRS studies can be conducted on both awake (as in Taga et al.[36]) and resting/sleeping (as in Karen et al.[30] and the current study) infants. It is unclear whether sleep state can also affect the neurovascular response. While electrophysiology studies of visual evoked potentials have shown differences in the latency and amplitude of the electrical response between sleeping and awake infants,[41,42] no clear evidence is available to show an effect on the hemodynamic response. While the cited NIRS results seem to report similar visual response patterns regardless of the level of consciousness, to our knowledge, no randomized controlled NIRS study has investigated the effect of behavioral states and sedation on the visual activation pattern.

It has been hypothesized that maturation or development of the neurovascular coupling may modulate the activation patterns observed in infants.[20,26,30,38] Increasing white matter myelination at 8 weeks of age with an increase in metabolic demand was proposed by Yamada et al. to explain the negative BOLD response seen in older infants.[20] In studies that recruited a higher percentage of infants that had been born preterm, a higher percentage of infants were seen with an inverted functional response to visual stimulation later in life,[20,26] suggesting that prematurity may also affect subsequent cerebral metabolism and should be controlled. To resolve these ambiguities, it is crucial for studies to be tightly controlled in both gestational age range and clinical course. For this reason, we restricted ourselves to studying healthy term-born infants within only the first three days of life. While there are changes in baseline cerebral hemodynamics during this time window, this is a tight timing constraint relative to

the existing literature. Our findings show a functional response pattern similar to that of adults. By qualitative visual inspection, it does appear that the response is slower in the infants than the adults; however, a more detailed study with great numbers of infants and adults would be needed to quantitatively evaluate the potential timing difference.

While the proposed superficial signal regression method improves the reliability of infant data, further optimization is possible. The superficial noise signal is produced from the most closely spaced SD pairs. These SD pairs are separated by 1 cm, giving the signal an approximately 3-mm penetration depth. We have found that in some infants the 1-cm spacing is sufficient to sample brain signals. In the case where the functional brain signal is mixed in with the physiological noise signal, the regression may reduce the intensity of the brain signal in addition to reducing the noise. As a result, the contrast is degraded. Alternative solutions, such as independent component analysis (ICA), might allow for better removal of noise sources that are present in all channels.[43] In addition, extension of the imaging cap to a larger field of view will provide more robust imaging data. In adults, where larger fields have been used, the spatial localization of the response has provided further improvements in contrast to noise ratio. The potential for these proposed improvements in data analysis and instrumentation, along with further optimization and expansion of the stimulation paradigm, suggest that while there is yet work to be done, it is reasonable to foresee a robust protocol emerging for routine clinical use.

Resolving the controversy over the true neurovascular coupling in infants has been challenging. Our results show that in newborn healthy term infants in the first three days of life during a visual stimulus, there is an increase in HbO_2 and a decrease in HbR. This pattern of visual response is similar to our adult data, as well as some recently published findings in infants, suggesting that the visual activation response for infants at term is similar to the mature response. Since the age, behavioral/conscious state, and visual stimulation paradigm all may alter the neurovascular response, we aimed to control these variables in our study. We believe that the use of NIRS provides a crucial insight into the hemodynamics that is not found with BOLD-fMRI, and further, that the high-density NIRS technique with superficial signal regression provides a more reliable measurement of brain hemodynamics than typically afforded by traditional NIRS systems. Future research can use the flexible techniques proposed here to analyze longitudinal variations that may occur in the neurovascular coupling of infants. Establishing a firm understanding of the normal hemodynamic response in healthy infants is a critical first step toward evaluating abnormal responses in high-risk infants to aid clinicians in the early recognition of cerebral dysfunction.

Acknowledgments

This work was supported in part by the following research grants: R21-EB007924 (Culver), R21 HD057512 (Culver), and T90-DA022871 (White).

References

1. S. Saigal and L. W. Doyle, "Preterm birth 3—an overview of mortality and sequelae of preterm birth from infancy to adulthood," *Lancet* **371**(9608), 261–269 (2008).
2. B. W. Zeff, B. R. White, H. Dehghani, B. L. Schlaggar, and J. P. Culver, "Retinotopic mapping of adult human visual cortex with high-density diffuse optical tomography," *Proc. Natl. Acad. Sci. U.S.A.* **104**(29), 12169–12174 (2007).
3. H. Obrig and A. Villringer, "Beyond the visible—Imaging the human brain with light," *J. Cereb. Blood Flow Metab.* **23**(1), 1–18 (2003).
4. A. Y. Bluestone, G. Abdoulaev, C. H. Schmitz, R. L. Barbour, and A. H. Hielscher, "Three-dimensional optical tomography of hemodynamics in the human head," *Opt. Express* **9**(6), 272–286 (2001).
5. A. P. Gibson, T. Austin, N. L. Everdell, M. Schweiger, S. R. Arridge, J. H. Meek, J. S. Wyatt, D. T. Delpy, and J. C. Hebden, "Three-dimensional whole-head optical passive motor evoked responses in the tomography of neonate," *Neuroimage* **30**(2), 521–528 (2006).
6. D. K. Joseph, T. J. Huppert, M. A. Franceschini, and D. A. Boas, "Diffuse optical tomography system to image brain activation with improved spatial resolution and validation with functional magnetic resonance imaging," *Appl. Opt.* **45**(31), 8142–8152 (2006).
7. M. E. Raichle and M. A. Mintun, "Brain work and brain imaging," *Annu. Rev. Neurosci.* **29**, 449–476 (2006).
8. D. J. Heeger, A. C. Huk, W. S. Geisler, and D. G. Albrecht, "Spikes versus BOLD: what does neuroimaging tell us about neuronal activity?" *Nature Neurosci.* **3**(7), 631–633 (2000).
9. N. Fujiwara, K. Sakatani, Y. Katayama, Y. Murata, T. Hoshino, C. Fukaya, and T. Yamamoto, "Evoked-cerebral blood oxygenation changes in false-negative activations in BOLD contrast functional MRI of patients with brain tumors," *Neuroimage* **21**(4), 1464–1471 (2004).
10. B. Bonakdarpour, T. B. Parrish, and C. K. Thompson, "Hemodynamic response function in patients with stroke-induced aphasia: implications for fMRI data analysis," *Neuroimage* **36**, 322–331 (2007).
11. P. Zou, R. K. Mulhern, R. W. Butler, C.-S. Li, J. W. Langston, and R. J. Ogg, "BOLD responses to visual stimulation in survivors of childhood cancer," *Neuroimage* **24**(1), 61–69 (2005).
12. C. Iadecola, "Neurovascular regulation in the normal brain and in Alzheimer's disease," *Nat. Rev. Neurosci.* **5**(5), 347–360 (2004).
13. M. D'Esposito, L. Y. Deouell, and A. Gazzaley, "Alterations in the bold FMRI signal with ageing and disease: a challenge for neuroimaging," *Nat. Rev. Neurosci.* **4**(11), 863–872 (2003).
14. M. T. Colonnese, M. A. Phillips, M. Constantine-Paton, K. Kaila, and A. Jasanoff, "Development of hemodynamic responses and functional connectivity in rat somatosensory cortex," *Nat. Neurosci.* **11**(1), 72–79 (2008).
15. P. Born, H. Leth, M. J. Miranda, E. Rostrup, A. Stensgaard, B. Peitersen, H. B. W. Larsson, and H. C. Lou, "Visual activation in infants and young children studied by functional magnetic resonance imaging," *Pediatr. Res.* **44**(4), 578–583 (1998).
16. A. P. Born, E. Rostrup, M. J. Miranda, H. B. W. Larsson, and H. C. Lou, "Visual cortex reactivity in sedated children examined with perfusion MRI (FAIR)," *Magn. Reson. Imaging* **20**(2), 199–205 (2002).
17. A. P. Born, M. J. Miranda, E. Rostrup, P. B. Toft, B. Peitersen, H. B. W. Larsson, and H. C. Lou, "Functional magnetic resonance imaging of the normal and abnormal visual system in early life," *Neuropediatrics* **31**(1), 24–32 (2000).
18. S. G. Erberich, A. Panigrahy, P. Friedlich, I. Seri, M. D. Nelson, and F. Gilles, "Somatosensory lateralization in the newborn brain," *Neuroimage* **29**(1), 155–161 (2006).
19. S. G. Erberich, P. Friedlich, I. Seri, M. D. Nelson, and S. Bluml, "Functional MRI in neonates using neonatal head coil and MR compatible incubator," *Neuroimage* **20**(2), 683–692 (2003).
20. H. Yamada, N. Sadato, Y. Konishi, S. Muramoto, K. Kimura, M. Tanaka, Y. Yonekura, Y. Ishii, and H. Itoh, "A milestone for normal development of the infantile brain detected by functional MRI," *Neurology* **55**(2), 218–223 (2000).
21. J. Steinbrink, A. Villringer, F. C. D. Kempf, D. Haux, S. Boden, and H. Obrig, "Illuminating the BOLD signal: combined fMRI-fNIRS studies," *Magn. Reson. Imaging* **24**(4), 495–505 (2006).
22. J. P. Culver, A. M. Siegel, M. A. Franceschini, J. B. Mandeville, and D. A. Boas, "Evidence that cerebral blood volume can provide brain activation maps with better spatial resolution than deoxygenated hemoglobin," *Neuroimage* **27**, 947–959 (2005).
23. A. K. Dunn, A. Devor, H. Bolay, M. L. Andermann, M. A. Moskowitz, A. M. Dale, and D. A. Boas, "Simultaneous imaging of total cerebral hemoglobin concentration, oxygenation, and blood flow during functional activation," *Opt. Lett.* **28**(1), 28–30 (2003).
24. D. A. Boas, G. Strangman, J. P. Culver, R. D. Hoge, G. Jasdzewski,

R. A. Poldrack, B. R. Rosen, and J. B. Mandeville, "Can the cerebral metabolic rate of oxygen be estimated with near-infrared spectroscopy?" *Phys. Med. Biol.* **48**(15), 2405–2418 (2003).
25. S. Muramoto, H. Yamada, N. Sadato, H. Kimura, Y. Konishi, K. Kimura, M. Tanaka, T. Kochiyama, Y. Yonekura, and H. Ito, "Age-dependent change in metabolic response to photic stimulation of the primary visual cortex in infants: functional magnetic resonance imaging study," *J. Comput. Assist. Tomogr.* **26**(6), 894–901 (2002).
26. T. Kusaka, K. Kawada, K. Okubo, K. Nagano, M. Namba, H. Okada, T. Imai, K. Isobe, and S. Itoh, "Noninvasive optical imaging in the visual cortex in young infants," *Hum. Brain Mapp* **22**(2), 122–132 (2004).
27. R. B. Saager and A. J. Berger, "Direct characterization and removal of interfering absorption trends in two-layer turbid media," *J. Opt. Soc. Am. A Opt. Image Sci. Vis* **22**(9), 1874–1882 (2005).
28. A. Duncan, J. H. Meek, M. Clemence, C. E. Elwell, P. Fallon, L. Tyszczuk, M. Cope, and D. T. Delpy, "Measurement of cranial optical path length as a function of age using phase resolved near infrared spectroscopy," *Pediatr. Res.* **39**(5), 889–894 (1996).
29. S. Wray, M. Cope, and D. T. Delpy, "Characteristics of the near infrared absorption spectra of cytochrome aa3 and hemoglobin for the noninvasive monitoring of cerebral oxygenation," *Biochim. Biophys. Acta* **933**, 184–192 (1988).
30. T. Karen, G. Morren, D. Haensse, A. S. Bauschatz, H. U. Bucher, and M. Wolf, "Hemodynamic response to visual stimulation in newborn infants using functional nean-infrared spectroscopy," *Hum. Brain Mapp* **29**(4), 453–460 (2008).
31. J. S. Wyatt, M. Cope, D. T. Delpy, P. van der Zee, S. Arridge, A. D. Edwards, and E. O. R. Reynolds, "Measurement of optical path length for cerebral near-infrared spectroscopy in newborn infants," *Dev. Neurosci.* **12**, 140–144 (1990).
32. M. A. Franceschini, S. Thaker, G. Themelis, K. K. Krishnamoorthy, H. Bortfeld, S. G. Diamond, D. A. Boas, K. Arvin, and P. E. Grant, "Assessment of infant brain development with frequency-domain near-infrared spectroscopy," *Pediatr. Res.* **61**(5), 546–551 (2007).
33. P. E. Grant, N. Roche-Labarbe, A. Surova, G. Themelis, J. Selb, E. K. Warren, K. S. Krishnamoorthy, D. A. Boas, and M. A. Franceschini, "Increased cerebral blood volume and oxygen consumption in neonatal brain injury," *J. Cereb. Blood Flow Metab.* **29**(10), 1704–1713 (2009).
34. G. Strangman, M. A. Franceschini, and D. A. Boas, "Factors affecting the accuracy of near-infrared spectroscopy concentration calculations for focal changes in oxygenation parameters," *Neuroimage* **18**(4), 865–879 (2003).
35. K. Uludag, J. Steinbrink, A. Villringer, and H. Obrig, "Separability and cross talk: optimizing dual wavelength combinations for near-infrared spectroscopy of the adult head," *Neuroimage* **22**(2), 583–589 (2004).
36. G. Taga, K. Asakawa, A. Maki, Y. Konishi, and H. Koizumi, "Brain imaging in awake infants by near-infrared optical topography," *Proc. Natl. Acad. Sci. U.S.A.* **100**(19), 10722–10727 (2003).
37. J. H. Meek, M. Firbank, C. E. Elwell, J. Atkinson, O. Braddick, and J. S. Wyatt, "Regional hemodynamic responses to visual stimulation in awake infants," *Pediatr. Res.* **43**(6), 840–843 (1998).
38. E. Martin, P. Joeri, T. Loenneker, D. Ekatodramis, D. Vitacco, J. Hennig, and V. L. Marcar, "Visual processing in infants and children studied using functional MRI," *Pediatr. Res.* **46**(2), 135–140 (1999).
39. V. L. Marcar, U. Schwarz, E. Martin, and T. Loenneker, "How depth of anesthesia influences the blood oxygenation level-dependent signal from the visual cortex of children," *Am. J. Neuroradiol.* **27**(4), 799–805 (2006).
40. A. F. Cannestra, S. Y. Bookheimer, N. Pouratian, A. O'Farrell, N. Sicotte, N. A. Martin, D. Becker, G. Rubino, and A. W. Toga, "Temporal and topographical characterization of language cortices using intraoperative optical intrinsic signals," *Neuroimage* **12**(1), 41–54 (2000).
41. P. Apkarian, "Temporal frequency responsivity shows multiple maturation phases: state-dependent visual evoked potential luminance flicker fusion from birth to 9 months," *Visual Neurosci.* **10**, 1007–1018 (1993).
42. E. Mercuri, K. v. Siebenthal, S. Tutuncuoglu, F. Guzzetta, and P. Casaer, "The effect of behavioral states on visual evoked responses in preterm and full-term newborns," *Neuropediatrics* **26**, 211–123 (1995).
43. J. Markham, B. R. White, B. W. Zeff, and J. P. Culver, "Blind identification of evoked human brain activity with independent component analysis of optical data," *Hum. Brain Mapp* **30**(8), 2382–2392 (2009).
44. T. Morita, T. Kochiyama, H. Yamada, Y. Konishi, Y. Yonekura, M. Matsumura, and N. Sadato, "Difference in the metabolic response to photic stimulation of the lateral geniculate nucleus and the primary visual cortex of infants: a fMRI study," *Neurosci. Res.* **38**, 63–70 (2000).
45. L. T. L. Sie, S. Rombouts, J. Valk, A. A. M. Hart, P. Scheltens, and M. S. van der Knaap, "Functional MRI of visual cortex in sedated 18 month-old infants with or without periventricular leukomalacia," *Dev. Med. Child Neurol.* **43**(7), 486–490 (2001).
46. N. R. Altman and B. Bernal, "Brain activation in sedated children: auditory and visual functional MR imaging," *Radiology* **221**(1), 56–63 (2001).
47. H. Watanabe, F. Homae, T. Nakano, and G. Taga, "Functional activation in diverse regions of the developing brain of human infants," *Neuroimage* **43**(2), 346–357 (2008).
48. Y. Hoshi, I. Oda, Y. Wada, Y. Ito, Y. Yamashita, M. Oda, K. Ohta, Y. Yamada, and M. Tamura, "Visuospatial imagery is a fruitful strategy for the digit span backward task: a study with near-infrared optical tomography," *Cog. Brain Res.* **9**(3), 339–342 (2000).